07

Single-mode lasing on radial modes in ring-cavity quantum-cascade lasers

© A.V. Babichev[1], N.Yu. Kharin[2], E.S. Kolodeznyi[1], D.S. Papylev[1], D.A. Mikhailov[3], G.V. Voznyuk[3], M.I. Mitrofanov[3,4], V.V. Dyudelev[3], A.G. Gladyshev[1], S.O. Slipchenko[3], A.V. Lyutetsky[3], V.P. Evtikhiev[3], V.Yu. Panevin[2], L.Ya. Karachinsky[1], I.I. Novikov[1], G.S. Sokolovsky[3], N.A. Pikhtin[3], A.Yu. Egorov[1]

[1] ITMO University, St. Petersburg, Russia
[2] Peter the Great Saint-Petersburg Polytechnic University, St. Petersburg, Russia
[3] Ioffe Institute, St. Petersburg, Russia
[4] Submicron Heterostructures for Microelectronics, Research & Engineering Center, RAS, Saint-Petersburg, Russia
E-mail: a.babichev@mail.ioffe.ru

Received February 12, 2025
Revised March 4, 2025
Accepted March 12, 2025

The results of stable single-mode lasing in ring-cavity quantum-cascade lasers are presented. Slits of the second-order grating with etching depth varying along the ring cavity are formed by direct ion-beam lithography. Single-mode lasing at the wavelength of 7.65 μm with the signal-to-noise suppression ratio of 22–25 dB just above the lasing threshold has been obtained. Increasing the current pumping by 40 % leads to an increase in the side-mode suppression ratio up to 28 dB.

Keywords: superlattices, quantum-cascade laser, selective ring cavity, single-mode lasing, indium phosphide, direct ion-beam lithography.

DOI: 10.61011/TPL.2025.06.61290.20280

Surface-emitting single-mode quantum-cascade lasers (QCLs) are an alternative to long-wavelength vertical-cavity surface-emitting lasers [1–5] since they allow creating an array of vertically coupled lasers.

To date, results have been presented on the formation and study of output characteristics of surface-emitting QCLs designed as a photonic crystal [6], selective ring cavity [7–12], selective micro-ring cavity [13], and microstrip distributed-feedback lasers [14]. Unlike the photonic-crystal lasers [6], ring-cavity geometry allowed achieving lasing in the continuous-wave (CW) current pumping mode. Therewith, the maximum lasing temperature in the CW mode was 300 and 100–230 K for QCLs with the spectral range near 4.6 μm [12,15] and 8 μm [16,17], respectively. By using a buried QCL heterostructure and efficient AlN-based heat sink, the authors succeeded [12,15] in significantly reducing the laser thermal load and achieving for the first time the CW-mode room-temperature lasing. The CW-mode output optical power was 400 mW [15]; however, due to a significant coupling coefficient between the grating and active region, lasing corresponded to a high-order mode (61). For this reason, the authors of [15] failed to obtain lasing with the intensity maximum in the far-field center (the first maximum was located at the angle $2\theta = 12^\circ$). Transition to the design implying a complex coupling regime provided lasing on the fundamental mode with the output optical power of 202 mW; however, no intensity maximum in the far-field center was demonstrated in this case. To obtain a far-field central intensity maximum, a double „sharp“ (at 90 and 270° along the ring cavity) phase shift by π [18] is typically used. An alternative approach consists in applying a gradual phase shift (due to creating two gratings) by π with the slit width varying along the ring cavity. A similar phase shift may be provided by varying the grating slit etching depth.

This paper presents the first data on obtaining single-mode lasing in ring-cavity QCLs with the grating slit etching depth varying along the ring cavity.

The QCL heterostructure was grown by molecular beam epitaxy on a slightly doped indium phosphide substrate (with the dopant (sulfur) concentration of $(1-3) \cdot 10^{17}$ cm^{-3}). To create a 50-period cascade, the scheme implying two-phonon lower level depletion was used [19]. The roles of the lower and upper plates were played by the $In_{0.53}Ga_{0.47}As$ and InP layers 500 and 3900 nm thick with the doping levels of $5 \cdot 10^{16}$ and $1 \cdot 10^{17}$ cm^{-3}, respectively. The top (contact) layer was constructed based on $In_{0.53}Ga_{0.47}As$; its thickness was 120 nm, while the doping gradient ranged as $(1-100) \cdot 10^{17}$ cm^{-3}. Profile of the ring cavity 289 μm in average radius and 25 μm in width (near the contact layer) was formed by liquid etching 7 μm deep. The current pumping region width near the contact layer was 17 μm (see the inset in Fig. 1, *b*). Along with fabricating ring QCLs, there were created QCLs of the semi-ring type (of the similar radius) and strip type (with the cavity length of 1.7 mm and near-surface contact width of 20 μm) for the purpose of evaluating the output optical power.

Grating slits with variable etching depth may be formed using grayscale lithography techniques (direct laser, elec-

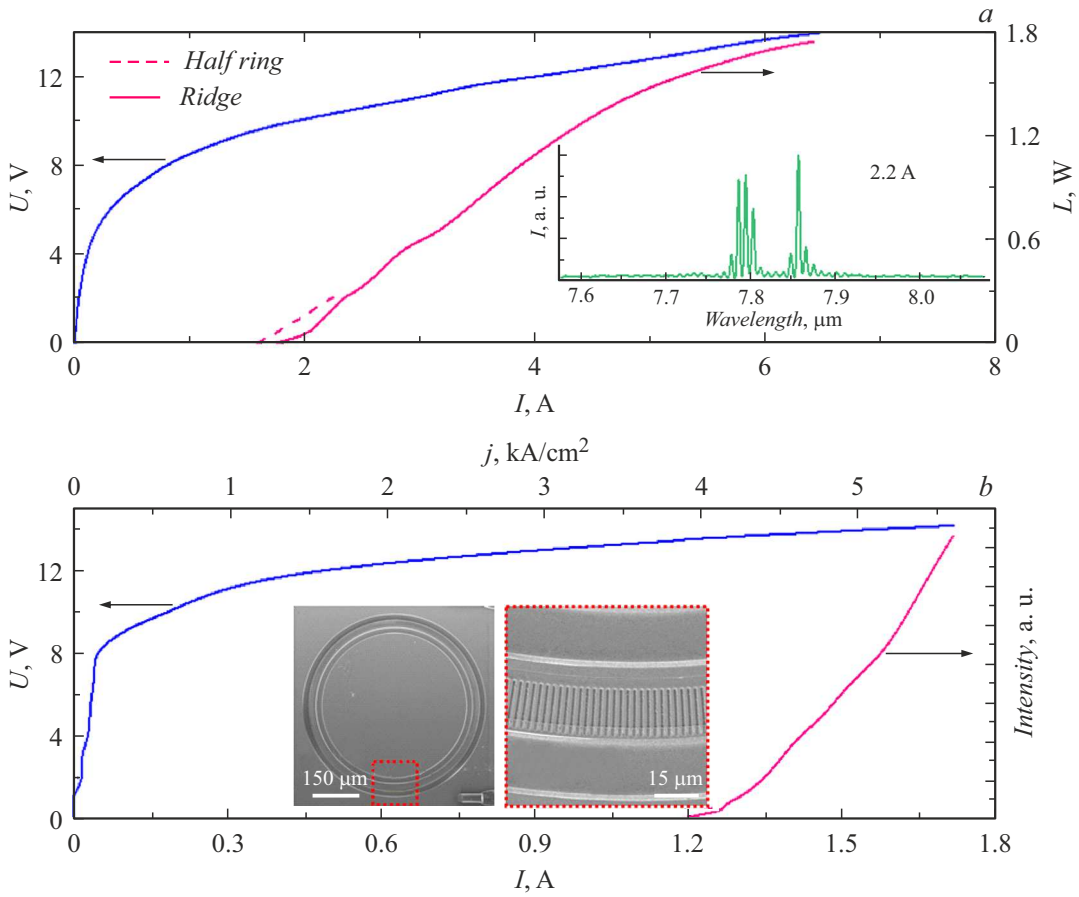

Figure 1. *a* — I-V and P-W characteristics of a semi-ring (dashed lines) and strip (solid lines) QCLs at 293 K. The presented output optical power was measured from both mirrors. The inset shows the lasing spectrum of a semi-ring QCL at 2.2 A. *b* — integrated radiation intensity versus current pumping and I-V characteristic of ring-cavity QCL at 83 K. The insets present the images of ring-cavity QCLs obtained by scanning electron microscopy.

tronic or X-ray ones, or technique of glass masks whose transparency depends on the radiation dose) and direct ion lithography. Unlike the grayscale lithography, the direct ion lithography combines both the lithographic pattern formation and maskless etching. Using direct ion lithography, 767 slits of the second-order grating were etched with the period of 2.37 μm. The grating period was determined by the position of the semi-ring laser electroluminescence spectrum maximum (see the inset to Fig. 1, *a*). The slit etching depth increased while moving over the ring cavity surface. The minimum etching depth was ~ 605 nm and depended on the metallization thickness. The maximum slit etching depth was $\sim 4.41\,\mu$m. The grating slit transverse dimensions were $0.71 \times 16\,\mu$m. The under-exposure ion energy was 20 keV, operating current was 2 nA, beam step was 10 nm, and exposure time was 2 μs. The ion fluence varied in the range of $(6.25-20) \cdot 10^{17}$ cm^{-2}.

Lasing spectra of a ring-cavity QCL located in a cryostat were measured at 83 K using Fourier spectrometer Bruker Vertex 80v operating in the step-scan mode. Duration and repetition rate of the pump pulses were 150 ns and 15 kHz. Absolute output optical power of the semi-ring and strip QCLs was measured with power meter Thorlabs PM100/S401C.

The measured I-V and P-V characteristics of the semi-ring and strip QCLs are presented in Fig. 1, *a*. Output optical power of the semi-ring QCL was 270 mW with exceeding the threshold current by 40 %. The strip QCLś maximum output power was 1.7 W. Thus, we may state that the considered heterostructure design provides high output optical power.

Threshold current I_{th} was measured in the ring cavity (prior to the grating formation) and proved to be 1.67 A at 293 K. The measurements were taken from the cleaved sample face, as discussed previously [20,21]. Taking into account characteristic temperature $T_0 = 136$ K in the studied ring-cavity QCLs [22], the ring cavity threshold current at 83 K was estimated and appeared to be ~ 0.4 A. Formation of the selective ring cavity (grating slit etching) led to the I_{th} increase to 1.16 A which corresponds to threshold current density $j_{th} = 3.8$ kA/cm^2 (Fig. 1, *b*). Fig. 2 presents the measured single-mode lasing spectra at the current pumping level of up to 1.62 A. Stable (mode-hope-free) single-mode lasing is observed in the entire range

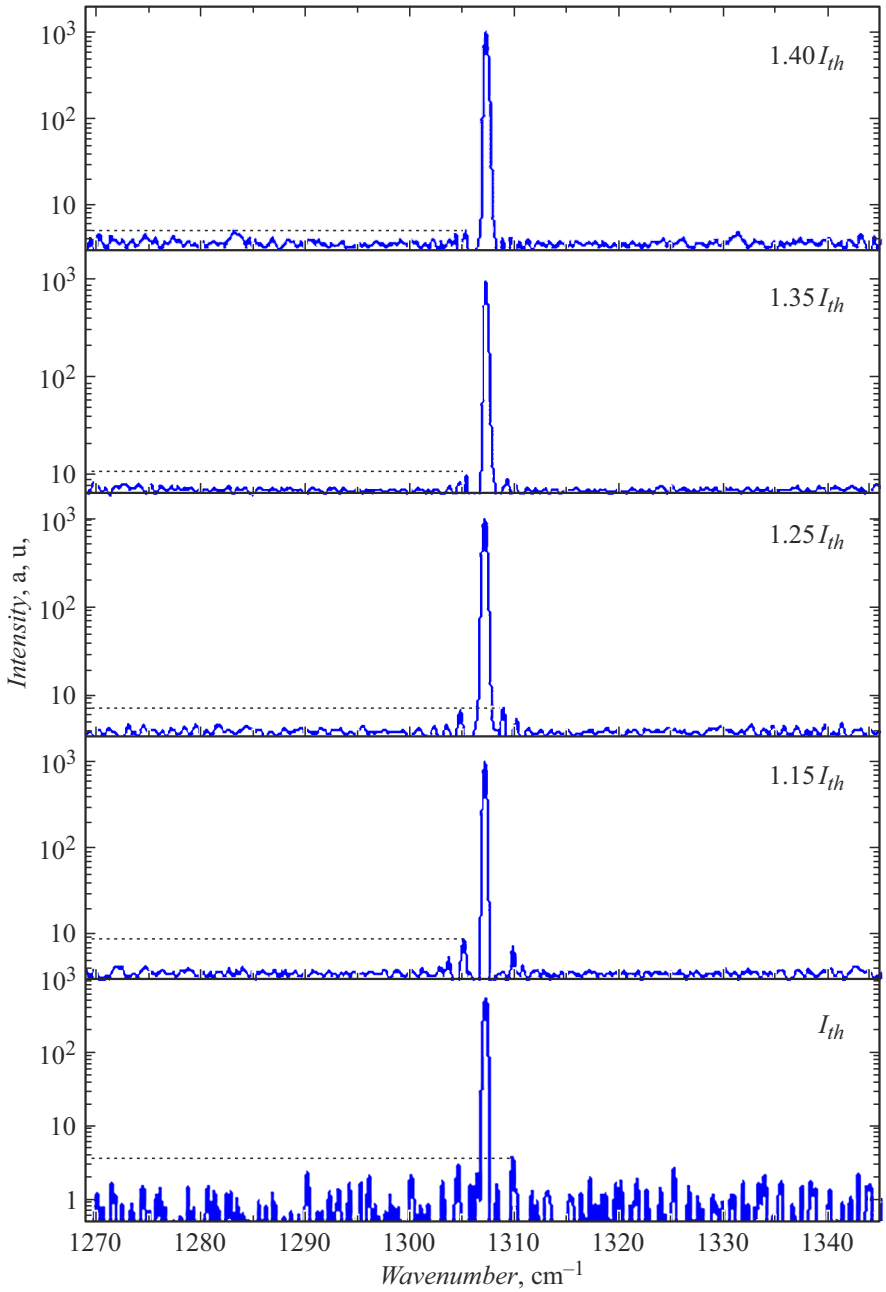

Figure 2. Spectra of single-mode lasing of a ring-cavity QCL at the temperature of 83 K for different current pumping levels.

under consideration. Single-mode lasing near the pumping threshold corresponds to the wavelength of 7.65 μm with the signal-to-noise ratio of 22–25 dB (Fig. 3). The current pumping increase by 40 % leads to an increase in the side-mode suppression ratio up to 28 dB. Previously, single-mode lasing (SMSR $\leqslant$ 25 dB) in a narrower dynamic range (up to $1.27I_{th}$) was demonstrated for a ring-cavity QCL of a smaller radius (191 μm) [10].

Analysis of a lasing line shift within the pump pulse duration was performed. At the pump level of $1.08I_{th}$, the lasing line shifts within the pulse duration by 0.22 cm^{-1}, while average line shifting rate υ within the pump pulse duration t (average value $\delta\upsilon/\delta t$) is $2.4 \cdot 10^{-3}$ cm$^{-1} \cdot$ ns^{-1}. The maximum lasing line shift during the pump pulse was 0.41 cm^{-1}, which corresponds to the pump level of $1.4I_{th}$. Average $\delta\upsilon/\delta t$ at the pump current density of 5.3 kA/cm^2 appears to be $2.7 \cdot 10^{-3}$ cm$^{-1} \cdot$ ns^{-1}. Average $d\upsilon/dt$ for QCL based on a selective ring cavity of a smaller radius (190 μm) was previously evaluated at the same threshold current density as $6.2 \cdot 10^{-3}$ cm$^{-1} \cdot$ ns^{-1} [23].

As the current pump level increases to $1.4I_{th}$, the initial lasing line shifts during the pump pulse by -0.035 cm^{-1}. Provided the rate of the lasing line position variation with temperature ($\delta\upsilon/\delta T$) for the QCL design under consideration (0.092 cm^{-1}/K) is taken into account [24], the estimate of the studied QCL heating does not exceed 0.4 K.

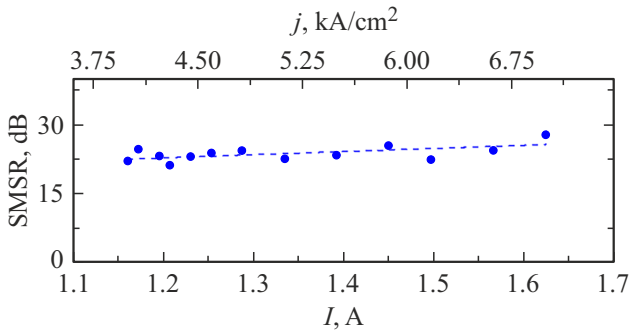

Figure 3. Side mode suppression coefficient versus the current pumping level.

To compare characteristics of single-mode lasers with the same geometric dimensions, lasing line shift $\Delta\upsilon$ with increasing current is used. In turn, in comparing lasers with different thermal loads, more correct is to assess the lasing line shifting with increasing pump current density $\Delta\upsilon/\Delta j$. Pump current density $\Delta\upsilon/\Delta j$ was estimated to be $0.099\,\mathrm{cm}^{-1}\cdot\mathrm{kA}^{-1}$. This value is consistent with that previously presented for single-mode strip lasers with the same heterostructure design ($\Delta\upsilon/\Delta j = 0.094\,\mathrm{cm}^{-1}\cdot\mathrm{kA}^{-1}$ [24]).

Thus, the paper presents the first results on obtaining single-mode lasing in a ring-cavity QCL with the variable grating slit etching depth. Comparison with the previously presented results for the ring-cavity QCL [10] showed that optimization of the grating slit etching depth made it possible to increase (up to $1.4I_{th}$) the current dynamic range where the single-mode lasing is observed. Average rate of the lasing line shift during the pump pulse (chirp) was estimated and appeared to be $2.7\cdot10^{-3}\,\mathrm{cm}^{-1}\cdot\mathrm{ns}^{-1}$ at the pump current density of $5.3\,\mathrm{kA/cm}^2$.

Funding

Studies performed by the authors from ITMO University concerning the laser characteristics were supported by the Russian Science Foundation, grant № 20-79-10285-P (https://rscf.ru/project/20-79-10285/).

Conflict of interests

The authors declare that they have no conflict of interests.

References

[1] A. Andrejew, S. Sprengel, M.-C. Amann, Opt. Lett., **41** (12), 2799 (2016). DOI: 10.1364/ol.41.002799
[2] G.K. Veerabathran, S. Sprengel, A. Andrejew, M.-C. Amann, Appl. Phys. Lett., **110** (7), 071104 (2017). DOI: 10.1063/1.4975813
[3] A. Simaz, G. Böhm, A. Köninger, M.A. Belkin, in *2024 IEEE 29th Int. Semiconductor Laser Conf. (ISLC)* (IEEE, 2024), p. 1–2. DOI: 10.1109/islc57752.2024.10717418
[4] A. Babichev, S. Blokhin, A. Gladyshev, L. Karachinsky, I. Novikov, A. Blokhin, M. Bobrov, N. Maleev, V. Andryushkin, E. Kolodeznyi, D. Denisov, N. Kryzhanovskaya, K. Voropaev, V. Ustinov, A. Egorov, H. Li, S.-C. Tian, S. Han, G. Sapunov, D. Bimberg, IEEE Photon. Technol. Lett., **35** (6), 297 (2023). DOI: 10.1109/lpt.2023.3241001
[5] S.A. Blokhin, A.V. Babichev, A.G. Gladyshev, L.Ya. Karachinsky, I.I. Novikov, A.A. Blokhin, M.A. Bobrov, N.A. Maleev, V.V. Andryushkin, D.V. Denisov, K.O. Voropaev, I.O. Zhumaeva, V.M. Ustinov, A.Yu. Egorov, N.N. Ledentsov, IEEE J. Quantum Electron., **58** (2), 2400115 (2022). DOI: 10.1109/jqe.2022.3141418
[6] Z. Wang, Z. Wang, Y. Liang, B. Meng, Y.-T. Sun, G. Omanakuttan, E. Gini, M. Beck, I. Sergachev, S. Lourdudoss, J. Faist, G. Scalari, Opt. Express, **27** (16), 22708 (2019). DOI: 10.1364/oe.27.022708
[7] G. Marschick, S. Isceri, R. Szedlak, H. Moser, J.P. Waclawek, E. Arigliani, R. Weih, W. Schrenk, G. Strasser, B. Hinkov, A. Maxwell Andrews, B. Lendl, B. Schwarz, APL Photon., **9** (10), 100806 (2024). DOI: 10.1063/5.0221189
[8] G. Marschick, J. Pelini, T. Gabbrielli, F. Cappelli, R. Weih, H. Knötig, J. Koeth, S. Höfling, P. De Natale, G. Strasser, S. Borri, B. Hinkov, ACS Photon., **11** (2), 395 (2024). DOI: 10.1021/acsphotonics.3c01159
[9] H. Knötig, B. Hinkov, R. Weih, S. Höfling, J. Koeth, G. Strasser, Appl. Phys. Lett., **116** (13), 131101 (2020). DOI: 10.1063/1.5139649
[10] A. Babichev, E. Kolodeznyi, A. Gladyshev, N. Kharin, V. Panevin, V. Shalygin, G. Voznyuk, M. Mitrofanov, S. Slipchenko, A. Lyutetskii, V. Evtikhiev, L. Karachinsky, I. Novikov, N. Pikhtin, A. Egorov, J. Opt. Technol., **90** (8), 422 (2023). DOI: 10.1364/jot.90.000422
[11] S. Kacmoli, C.F. Gmachl, Appl. Phys. Lett., **124** (1), 010502 (2024). DOI: 10.1063/5.0180606
[12] D.H. Wu, M. Razeghi, APL Mater., **5** (3), 035505 (2017). DOI: 10.1063/1.4978810
[13] D. Stark, M. Beck, J. Faist, APL Photon., **10** (1), 016122 (2025). DOI: 10.1063/5.0245311
[14] D. Stark, F. Kapsalidis, S. Markmann, M. Bertrand, B. Marzban, E. Gini, M. Beck, J. Faist, Laser Photon. Rev., **18** (8), 2300663 (2024). DOI: 10.1002/lpor.202300663
[15] Y. Bai, S. Tsao, N. Bandyopadhyay, S. Slivken, Q.Y. Lu, D. Caffey, M. Pushkarsky, T. Day, M. Razeghi, Appl. Phys. Lett., **99** (26), 261104 (2011). DOI: 10.1063/1.3672049
[16] B. Hinkov, J. Hayden, R. Szedlak, P. Martin-Mateos, B. Jerez, P. Acedo, G. Strasser, B. Lendl, Opt. Express, **27** (10), 14716 (2019). DOI: 10.1364/oe.27.014716
[17] E. Mujagić, M. Nobile, H. Detz, W. Schrenk, J. Chen, C. Gmachl, G. Strasser, Appl. Phys. Lett., **96** (3), 031111 (2010). DOI: 10.1063/1.3292021
[18] R. Szedlak, M. Holzbauer, D. MacFarland, T. Zederbauer, H. Detz, A.M. Andrews, C. Schwarzer, W. Schrenk, G. Strasser, Sci. Rep., **5** (1), 16668 (2015). DOI: 10.1038/srep16668
[19] L. Boulley, T. Maroutian, P. Goulain, A. Babichev, A. Egorov, L. Li, E. Linfield, R. Colombelli, A. Bousseksou, AIP Adv., **13** (1), 015315 (2023). DOI: 10.1063/5.0111159
[20] M. Piccardo, B. Schwarz, D. Kazakov, M. Beiser, N. Opačak, Y. Wang, S. Jha, J. Hillbrand, M. Tamagnone, W.T. Chen, A.Y. Zhu, L.L. Columbo, A. Belyanin, F. Capasso, Nature, **582** (7812), 360 (2020). DOI: 10.1038/s41586-020-2386-6

[21] N.Yu. Kharin, A.V. Babichev, D.A. Mikhailov, E.S. Kolodeznyi, V.V. Dudelev, V.Yu. Panevin, G. Voznyuk, M. Mitrofanov, S.O. Slipchenko, A.V. Lyutetskii, V.P. Evtikhiev, L.Ya. Karachinsky, I.I. Novikov, G.S. Sokolovskii, N.A. Pikhtin, A.Yu. Egorov, in *2024 Int. Conf. on Electrical Engineering and Photonics (EexPolytech)* (IEEE, 2024), p. 394–397. DOI: 10.1109/eexpolytech62224.2024.10755618

[22] D.S. Papylev, E.S. Kolodeznyi, A.V. Babichev, N.Yu. Kharin, G.V. Voznyuk, M.I. Mitrofanov, S.O. Slipchenko, A.V. Lyutetskii, V.P. Evtikhiev, L.Ya. Karachinsky, I.I. Novikov, V.Yu. Panevin, N.A. Pikhtin, A.Yu. Egorov, St. Petersburg Polytech. Univ. J.: Phys. Math., **17** (3.2), 71 (2024). DOI: 10.18721/JPM.173.213

[23] M. Brandstetter, A. Genner, C. Schwarzer, E. Mujagic, G. Strasser, B. Lendl, Opt. Express, **22** (3), 2656 (2014). DOI: 10.1364/oe.22.002656

[24] A.V. Babichev, E.S. Kolodeznyi, A.G. Gladyshev, D.V. Denisov, N.Yu. Kharin, A.D. Petruk, V.Yu. Panevin, S.O. Slipchenko, A.V. Lyutetskii, L.Ya. Karachinsky, I.I. Novikov, N.A. Pikhtin, A.Yu. Egorov, Tech. Phys. Lett., **48** (3), 6 (2022). DOI: 10.21883/TPL.2022.03.52872.19050.

Translated by EgoTranslating